



Design study of 10 kW superconducting generator for wind turbine applications

Abrahamsen, Asger Bech; Mijatovic, Nenad; Seiler, Eugen; Sørensen, Mads Peter; Koch, Martin; Nørgård, Per Bromand; Pedersen, Niels Falsig; Træholt, Chresten; Andersen, Niels Hessel; Østergaard, Jacob

Published in:
IEEE Transactions on Applied Superconductivity

Link to article, DOI:
[10.1109/TASC.2009.2017697](https://doi.org/10.1109/TASC.2009.2017697)

Publication date:
2009

Document Version
Publisher's PDF, also known as Version of record

[Link back to DTU Orbit](#)

Citation (APA):
Abrahamsen, A. B., Mijatovic, N., Seiler, E., Sørensen, M. P., Koch, M., Nørgård, P. B., Pedersen, N. F., Træholt, C., Andersen, N. H., & Østergaard, J. (2009). Design study of 10 kW superconducting generator for wind turbine applications. *IEEE Transactions on Applied Superconductivity*, 19(3), 1678-1682.
<https://doi.org/10.1109/TASC.2009.2017697>

General rights

Copyright and moral rights for the publications made accessible in the public portal are retained by the authors and/or other copyright owners and it is a condition of accessing publications that users recognise and abide by the legal requirements associated with these rights.

- Users may download and print one copy of any publication from the public portal for the purpose of private study or research.
- You may not further distribute the material or use it for any profit-making activity or commercial gain
- You may freely distribute the URL identifying the publication in the public portal

If you believe that this document breaches copyright please contact us providing details, and we will remove access to the work immediately and investigate your claim.

Design Study of 10 kW Superconducting Generator for Wind Turbine Applications

A. B. Abrahamsen, N. Mijatovic, E. Seiler, M. P. Sørensen, M. Koch, P. B. Nørgård, N. F. Pedersen, C. Træholt, N. H. Andersen, and J. Østergård

Abstract—We have performed a design study of a 10 kW superconducting slow rotating generator suitable for demonstration in a small scale wind turbine, where the drive train only consists of the turbine blades connected directly to the generator. The flux density in the superconducting rotor is chosen as $B = 1$ Tesla to be similar to the performance of permanent magnets and to represent a layout, which can be scaled up in future off-shore wind turbines. The proposed generator is a 8 pole synchronous machine based on race-track coils of high temperature superconducting tapes and an air cored copper stator enclosed in an iron shield.

Index Terms—Superconductivity, synchronous generator, wind turbines.

I. INTRODUCTION

THE challenges of future energy demand and the possible global warming due to fossil fuel consumption have increased the interest of large-scale use of wind turbines for electricity production. Most present turbines are operated on-shore, but the interference with the residents and higher wind speeds at sea is the motivation for building off-shore wind farms. A major fraction of the cost of off-shore farms is due to the foundations of the turbines, the grid connection and maintenance. Thus there is an incentive to place large turbines at sea and power ratings of 10 MW are desirable in 10 years. A superconducting generator might be advantageous for 10 MW turbines, because the weight and volume can be reduced compared to a conventional generator and thereby simplifying the turbine design. The gearbox of present turbines can also be omitted by utilizing a multi-pole generator which is driven directly by the turbine rotor. We have done a design study of a 10 kW direct driven multi-pole superconducting generator, which can be installed in a small wind tur-

bine and used to evaluate the robustness of the superconducting technology in a wind turbine environment, before the generator is scaled up by 3 orders of magnitude to the large scale turbines.

II. SMALL SCALE WIND TURBINES

Small wind turbines are commercially available and a wind turbine from Gaia-Wind [1] is operated at Risø -DTU [2]. It is a stall regulated turbine with a conventional drive train consisting of a gearbox and a fast rotating asynchronous generator with a power rating of 11 kW. This technology represents the first generation of drive trains, but direct driven synchronous generators based on permanent magnets such as $\text{Nd}_2\text{Fe}_{14}\text{B}$ have recently been introduced even in small scale turbines [3]. A superconducting direct driven synchronous generator will represent a third generation of drive trains for wind turbines, since superconducting coils are expected to provide magnetic flux densities exceeding the operation flux densities of the permanent magnets. The specifications of a superconducting generator for a small scale wind turbine are outlined according to the properties of the Gaia wind turbine. A wind turbine converts the kinetic energy of the wind into electric energy and the power of the wind P_{wind} is ideally given by [4]

$$P_{\text{wind}} = \frac{1}{2} \rho v_0^3 A_{\text{rotor}} C_P \quad (1)$$

where ρ is the density of the air, v_0 is the average wind speed, $A_{\text{rotor}} = \pi R_{\text{rotor}}^2$ is the rotor area swept by the blades with a length of R_{rotor} and C_P is the power coefficient, which is determined by the aerodynamic properties of the rotor and is related to the number of blades, the shape of the blade and the blade angle with respect to the incoming wind. The power coefficient determines the fraction of the available kinetic energy, which is transformed into torque on the turbine shaft. It is often given as function of the ratio λ between the blade tip speed v_T and the wind speed v_0

$$\lambda = \frac{v_T}{v_0} = \frac{R_{\text{rotor}} \omega}{v_0} \quad (2)$$

where Ω is the angular speed related to the rotor frequency by $\Omega = 2\pi f_{\text{rotor}}$.

The available wind power and the power curve of the Gaia turbine is shown on Fig. 1 as function of the average wind speed v_0 . The C_P curve has been plotted by assuming a constant rotation speed of 56 Revolutions Per Minute (rpm) and $R_{\text{rotor}} = 6.5$ m. It is seen that the nominal 11 kW power production is first reached when the wind speed exceeds the nominal wind speed of $v_0 = 9.5$ m/s. The Gaia wind turbine illustrate how the stall

Manuscript received August 26, 2008. First published June 05, 2009; current version published July 15, 2009. This work was supported in part by the Technical University of Denmark under the globalization funded project superwind.dk

A. B. Abrahamsen, E. Seiler, and N. H. Andersen are with the Materials Research Division, Risø National Laboratory for Sustainable Energy, Technical University of Denmark, DK-4000 Roskilde, Denmark (e-mail: asab@risoe.dtu.dk; eugen.seiler@risoe.dk; niels.hessel@risoe.dk).

N. Mijatovic, M. Koch, N. F. Pedersen, C. Træholt, and J. Østergård are with the Department of Electrical Engineering, Technical University of Denmark, DK-2800 Lyngby, Denmark (e-mail: nm@elektro.dtu.dk; mk@oersted.dtu.dk; nfp@oersted.dtu.dk; ctr@oersted.dtu.dk; joe@oersted.dtu.dk).

M. P. Sørensen is with the Department of Mathematics, Technical University of Denmark, DK-2800 Lyngby, Denmark (e-mail: M.P.Sørensen@mat.dtu.dk).

P. B. Nørgård is with the Wind Energy Division, Risø National Laboratory for sustainable energy, Technical University of Denmark, DK-4000 Roskilde, Denmark (e-mail: joe@oersted.dtu.dk).

Digital Object Identifier 10.1109/TASC.2009.2017697

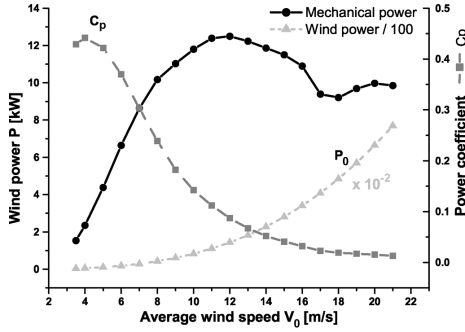


Fig. 1. Mechanical power curve P_{wind} of a small wind turbine as function the average wind speed when operated at a constant rotation speed of 56 rpm [2]. The wind power $P_0 = (1/2)\rho v_0^3 A_{rotor}$ available at the rotor is scaled by a factor 10^{-2} and is shown as well as the power coefficient C_P of the 2 blade rotor. A maximum of the available mechanical power $P_{wind} = P_0 C_P$ of the rotor is seen at intermediate wind speed due to the stall limitation of C_P .

regulation is obtained by the aerodynamic properties of the rotor and the rotation speed is fixed by the frequency of the electricity grid down scaled by the conversion factor of the gearbox. The available space in the nacelle is approximately a diameter of $D_{nacelle} = 0.8$ m and a length of $L = 1.0$ m. Large turbines today are pitch regulated by controlling the blade angle with respect to the incoming wind direction, whereby different power curves can be chosen. Additionally it becomes more common to decouple the generator frequency from the grid frequency by passing all the power of the turbine through power electronics consisting of two back-to-back coupled AC/DC converters. The generator of such a system can be of the synchronous type with the rotation speed controlled by the power electronics and this is also assumed to be the case for future superconducting wind turbine generators.

III. ANALYTICAL GENERATOR MODEL

We will use the analytical description of an air-cored synchronous machine [5], [6] to determine the properties of a slow rotating generator suitable for a gearless drive train of the Gaia turbine. The problem is only considered in the two dimensional rotation plane of the cylindrical machine, whereby the magnetic flux density distribution $\mathbf{B}(\theta, \mathbf{r})$ can be determined from the axial component of the vector potential. A simple representation of the rotor and stator coils is obtained by introducing a sinusoidal turn distribution

$$\frac{d}{dl}n(\theta) = n_0 \sin(p\theta) \quad (3)$$

where θ is the angle around the machine circumference as shown in Fig. 2, p is the number of pole pairs and n_0 is the maximum winding density per circumference segment $dl = r_0 d\theta$. Thus $n(\theta)$ gives the winding distribution, where the thickness of the winding layer is varying as a sinus function and the sheet current distribution is obtained by multiplying by the current i in each wire, $I(\theta) = n(\theta)i$. However the sinusoidal turn distribution is often realized by a box distribution as illustrated on Fig. 2 and

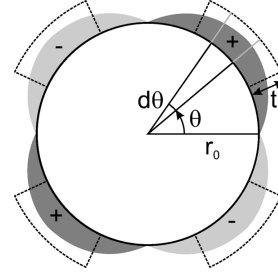


Fig. 2. Sinusoidal and box representation of turn distribution of rotor or stator winding of a 4 pole machine. The + and - sign refer to a current direction in and out of the paper. The turn distribution is assumed to be $n(\theta) = n_0 \sin(p\theta)$ where p is the number of pole pairs and n_0 is the turn density per circumference. Thus the equivalent sheet current is $I(\theta) = n(\theta)i$, where i is the current of each wire.

the prefactor of (3) is given by the first harmonic obtained from the Fourier transform of the box function.

The box function is specified as

$$n_b(\theta) = \begin{cases} n_{b0}, & \left| \frac{\pi}{2p} - \theta \right| < \delta\theta_b \\ -n_{b0}, & \left| -\frac{\pi}{2p} - \theta \right| < \delta\theta_b \end{cases} \quad (4)$$

where $\delta\theta$ is half of the opening angle of the box region. By assuming a constant winding density per area n_A then one can obtain the wire density per circumference segment $dl = r_0 d\theta$ from

$$n_{b0} = \frac{\int_{r_0}^{r_0+t} n_A r dr d\theta}{r_0 d\theta} = \frac{n_A t (t + 2r_0)}{2r_0} \quad (5)$$

where t is the winding layer thickness and r_0 is the radius of the winding support.

The Fourier coefficients b_k of the series representation $n(\theta) = \sum_{k=1}^{\infty} b_k \sin((k\pi\theta/\theta_{max}))$ with $\theta_{max} = \pi/p$ then becomes

$$b_k = \frac{1}{\theta_{max}} \int_{-\theta_{max}}^{\theta_{max}} n_b(\theta) \sin\left(\frac{k\pi\theta}{\theta_{max}}\right) d\theta \quad (6)$$

Thus the first harmonic ($k = 1$) of the box function becomes

$$b_1 = \frac{4}{\pi} n_{b0} \sin(p\delta\theta_b) = \frac{4}{\pi} n_{b0} k_w \quad (7)$$

where k_w is called the fundamental harmonic winding factor [5]. The sheet current distribution then becomes

$$\frac{d}{dl}i(\theta) = b_1 i \sin(p\theta) = A \sin(p\theta) \quad (8)$$

where A is the sheet current density in the unit $[A/m]$

$$A = b_1 i = \frac{4}{\pi} n_{b0} k_w i \quad (9)$$

A. Magnetic Flux Distribution

The flux distribution at r caused by the turn distribution (3) at r_0 and enclosed by an iron shield at r_{S2} has been derived analytically in [5]

$$\frac{B_r}{B_\theta} \Big\} = \frac{\mu_0 A}{2} \left(\frac{r_0}{r} \right)^{p+1} \left[1 + \eta \lambda_s \left(\frac{r}{r_{S2}} \right)^{2p} \right] \begin{Bmatrix} \cos(p\theta) \\ \sin(p\theta) \end{Bmatrix} \quad (10)$$

where μ_0 is the vacuum permeability and the square bracket is the enhancement factor due to the iron shield. The factor $\eta \lambda_s$ ranges between 0 and 1 in case of a fully saturated and infinitely permeable iron shield.

B. Machine Power

The output power of a synchronous machine consisting of a rotor and 3 stator turn distributions given by (3) at a radius r_R and r_S can now be calculated as

$$P = \frac{\pi^2}{\sqrt{2}} k_w B_{S0} A_s D^2 L_{gen} n_s \quad (11)$$

where B_{S0} is the peak radial flux density at the stator winding at r_S [6]. A_s is the sheet current of the 3-phase stator windings and $A_s = (3/2)A$ when the wire current i is an alternating current with root mean square amplitude i_{rms} . The stator diameter $D = 2r_S$ has been introduced, the effective length of the generator is L_{gen} and the rotation speed n_s is in [revolutions s^{-1}]. Thus the output power of a 10 kW machine consisting of a superconducting rotor and Cu stator inclosed in an iron shield can now be calculated from a box representation of the windings. We are aiming for a rotor field at the stator radius of the order $B_{S0} \sim 1$ T to match the magnetic flux density obtained by permanent magnets. The generator must fit into the nacelle giving a diameter $D = 0.56$ m and length of $L_{gen} = 0.4$ m. Finally a rotation speed of $n_s = 56 \text{ rpm}/60 \text{ s min}^{-1} = 0.93 \text{ s}^{-1}$ results in a stator sheet current density $A_s = 1.2 \cdot 10^4 \text{ Am}^{-1}$. The physical realization of such a machine is proposed below.

IV. GENERATOR LAYOUT

The coil geometry of a superconducting generator is restricted by the mechanical properties of the used superconducting wire and in the case of the ceramic high temperature superconductors (HTS) one can not bend the flat wires, which are often called tapes, on a diameter less than the critical bending diameter D_{cb} . Typical bending diameters of HTS tapes are $D_{cb, BiSCCO} = 50\text{--}70$ mm for the $\text{Bi}_2\text{Sr}_2\text{Ca}_2\text{Cu}_3\text{O}_{10+x}$ (Bi2223) tapes and $D_{cb, YBCO} = 25\text{--}35$ mm for $\text{YBa}_2\text{Cu}_3\text{O}_{6+x}$ (YBCO) coated conductors. The tape thickness $t_{tape} = 0.30\text{--}0.32$ mm is typical including 100 μm plastic insulation wrapped around the wire. The width of the tape is typically $w_{tape} = 4.3\text{--}4.5$ mm again including insulation. Thus the winding density of HTS tapes is typically, $n_A = 7.3 \cdot 10^5 \text{ m}^{-2}$. Coils of HTS tape is often wound in the form of a double pan-cake coil with an inner diameter larger than the critical bending diameter D_{cb} and a thickness equal to $2w_{tape}$.

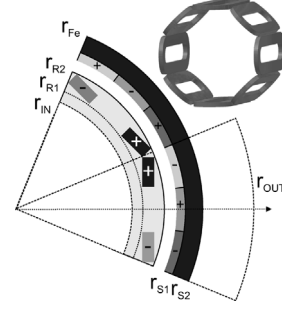


Fig. 3. Layout of 8 pole synchronous generator. The inner support structure spans from r_{in} and to the rotor between r_{R1} and r_{R2} . The stator windings of the 3-phases are spanned between r_{S1} and r_{S2} . An iron shield expands until r_{Fe} and the outer radius of the turbine nacelle is r_{out} . Inset: 3D representation of superconducting race-track rotor coils made of double pan-cake windings.

TABLE I
GENERATOR DIMENSIONS

Rotor	Stator
$r_{in} = 0.200$ m	$r_{S1} = 0.270$ m
$r_{R1} = 0.215$ m	$r_{S2} = 0.290$ m
$r_{R2} = 0.250$ m	$r_{Fe} = 0.320$ m

The superconducting rotor coils are based on the race-track geometry, where the strait section is assumed to be the effective length of the machine, $L_{gen} = 0.4$ m, and the inner opening of the coil is determined by the bending diameter of the HTS tapes $l_{air} = 0.08$ m $> D_{cb}$ as illustrated on Fig. 3. The frequency f of the generator voltage and current is related to the synchronous rotation speed ω and the number of pole pairs p in the generator $f = p\Omega/2\pi = 3.7$ Hz. Fig. 3 shows the 8 pole rotor coil geometry with each pole produced by a race-track coil consisting of two double pan-cakes. The thickness and width of the coil is $t_c = 2.0$ cm and $w_c = 5.0$ cm respectively. The positions of the rotor and stator windings are given in Table I, but the box representation of the rotor is assumed to span $r_{Rbox} = 0.223\text{--}0.243$ m and the opening angle is $\delta\theta_b = (\pi/2p)(2/3)$.

V. RESULTS AND DISCUSSION

The load line of the rotor coils is determined from the field and temperature dependent critical current $I_C(H, T)$ of different tapes [7]–[9] by calculating the resulting flux density in the rotor coil from (10) when the $I_C(H, T)$ at a certain field $\mu_0 H_0$ is inserted in the expression for the sheet current A given by (9). If the flux density produced by the coil exceeds the flux density used to determine the I_C then superconductivity is suppressed. Fig. 4 shows the maximum flux density along the θ direction in the rotor coil as function of the field used to determine I_C and the critical region is at the left of the dashed line. The θ component corresponds to the magnetic flux density perpendicular to the tape surface and will result in the lowest I_C due to the anisotropy of the critical current [10]. A safety margin of 50–80% of I_C must be applied to lower the probability of quenches of the rotor coils.

From Fig. 4 it is seen that the coated conductors will have a $B_{max} = 0.5\text{--}0.8$ Tesla corresponding to an $I_C = 50\text{--}120$ A

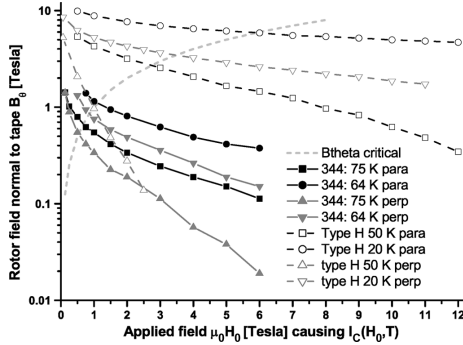


Fig. 4. Tangential magnetic flux density B_θ at the rotor winding given by (10) when inserting the field depend critical current $I_C(H_0, T)$ of different tapes into the expression for the rotor sheet current (9) (344 and Type H refer to coated conductors from American Superconductor and Bi-2223 tapes from Sumitomo respectively). The dashed line indicates the critical load line when the flux density of the coil exceeds the flux density specified by the critical current. Thus the operational load line of the rotor must be below the critical load line by a sufficient safety margin.

at $T = 75$ K and $T = 64$ K respectively. The large anisotropy of the Bi-2223 pinning properties makes operation at $T = 77$ K impossible due to the complete suppression of superconductivity when a magnetic flux component perpendicular to the tape is present. Thus a maximum flux density at the conductor of $B_{max} = 1\text{--}3$ T is possible with $I_C = 100\text{--}550$ A at $T = 50$ K and $T = 20$ K respectively. An operational engineering critical current of $J_e = 1.1 \cdot 10^4$ Acm $^{-2}$ is assumed to fulfil the safety margin and this will correspond to a wire current of $I = 150$ A. The corresponding sheet current (9) becomes $A_R = 2.5 \cdot 10^6$ Am $^{-1}$ and the maximum flux densities at the rotor coil and stator is predicted from (10) to become $|B|_{rotor,max} = 1.79$ T and $|B|_{stator,max} = 0.96$ T. Finite element calculation of the layout shown on Fig. 3 have confirmed the predicted flux densities and shows that the analytical box winding description is a good approximation of realistic superconducting coils.

A. Stator Properties

The current of one stator phase winding I_S can be determined by choosing a base voltage of $U_S = 400$ V/ $\sqrt{3} = 231$ V

$$P_{phase} = U_S I_S \Rightarrow I_S = \frac{P_{phase}}{U_S} = \frac{10 \text{ kW}/3}{231 \text{ V}} = 14.4 \text{ A} \quad (12)$$

By assuming a stator winding made of square copper wire with area $A_{Cu} = 5.3$ mm 2 then one can determine the wire area density needed to obtain a sufficient stator sheet current A_S . First A_S is calculated from the rotor flux density found in the previous section and the output power given by (11)

$$A_s = \frac{\sqrt{2}}{\pi^2} \frac{P}{k_w B_{S0} D^2 L_{gen} n_s} = 1.5 \cdot 10^4 \text{ Am}^{-1} \quad (13)$$

TABLE II
LENGTH AND WEIGHT OF GENERATOR COMPONENTS

Part	Length[m]	Weight [kg]
Rotor wire	7539	89 - 93
Rotor former	L = 0.66 m	73
Stator wire	2149	102
Iron	R = 0.29 \rightarrow 0.32 m & L = 0.4 m	181

The stator wire density is then determined from (5), (7) and (9) applied to the stator geometry

$$n_{A,S} = \frac{\pi}{2} \frac{\frac{2}{3} A_s r_{S1}}{t(t + 2r_{S1}) k_{w,S} I_s} = 1.0 \cdot 10^5 \text{ windings m}^{-2} \quad (14)$$

which correspond to approximately 20% of the stator area for epoxy. The resistance of the stator is estimated to be $R_S = 4.06 \Omega$ which will give a stator loss of $P_{Cu} = R_S I_S^2 = 842$ W and a stator efficiency of 0.92.

B. Wire Length and Generator Weight

The estimated length of the wires needed for the generator is shown in Table II. The weight has been estimated by assuming that the density of the HTC superconductor tapes is either equivalent to a 70/30 ratio of silver and Bi2223 or to pure nickel representing the coated conductors. Additionally the weight of the rotor support is estimated from the density of glass fiber. It is seen that the choice of a high rotor flux density comes at the price of a larger amount of superconductor in the rotor than copper in the stator. Thus from an economical point of view it would be desirable to replace some superconductor by Cu in the stator, but the present design is focused on demonstrating a superconducting coil layout, which can be scaled up to larger power ratings in future off-shore turbines. It is interesting to note that the total weight of Table II is $W_{total} = 449$ kg, which must be compared to 300 kg of gearbox and generator in the Gaia turbine. An increase of the drive train weight is often seen when changing to direct drive, but it is expected that the superconducting machines will become lighter than the conventional at high power ratings [11].

VI. CONCLUSION

We have shown a possible design of a direct driven 10 kW superconducting 8 pole synchronous generator based on 7.5 km of high temperature superconductor tape and that this generator might be demonstrated in a small scale wind turbine. An optimization of the generator is needed as a next step as well as the design of a cryogenic cooling system. The operation temperature will be determined by the trade off between higher engineering critical current density J_e at low temperatures and the power loss of the cooling system. However tapes with higher J_e would be needed if the operation temperature should be increased up to $T = 50$ K.

REFERENCES

- [1] (2008). Gaia-Wind A/S [Online]. Available: www.gaiawind.com
- [2] H. Bindner, P. A. C. Rosas, R. Teodorescu, and F. Blaabjerg, "Stand-Alone Version of the 11 kW Gaia Wind Turbine," 2004, ISBN 87-550-3376-8, Risø report: risø-R-1480 (EN).
- [3] Aircon GmbH & Co., Web-page [Online]. Available: www.aircon-international.com
- [4] T. Burton, D. Sharpe, N. Jenkins, and E. Bossanyi, *Wind Energy Handbook*. New York: Wiley, 2001, ISBN 0471489972.
- [5] A. Hughes and T. J. E. Miller, "Analysis of fields and inductances in air-cored and iron-cored synchronous machines.," *Proc. IEE*, vol. 124, no. 2, pp. 121–126, 1977.
- [6] T. J. E. Miller and A. Hughes, "Comparative design and performance of air-cored and iron-cored synchronous machines," *Proc. IEE*, vol. 124, no. 2, pp. 127–132, 1977.
- [7] M. W. Rupich, U. Shoops, D. T. Verebelyi, and C. L. H. Thieme *et al.*, "The development of second generation HTS wire at American Superconductors," *IEEE Trans. Appl. Supercond.*, vol. 17, no. 2, pp. 3379–3382, Mar. 2007.
- [8] N. Ayai, M. Kikuchi, K. Yamazaki, and S. Kobayashi *et al.*, "The Bi-2223 superconducting wires with 200A-class critical current," *IEEE Trans. Appl. Supercond.*, vol. 17, no. 2, pp. 3075–3078, Mar. 2007.
- [9] (2007). Sumitomo Electric. [Online]. Available: www.sei.co.jp/super/hts_e/index.html
- [10] R. Foltyn, L. Civale, L. MacManus-Driscoll, X. Jia, B. Maiorov, H. Wang, and M. Maley, "Materials science challenges for high-temperature superconducting wire," *Nature Materials*, vol. 6, p. 631, 2007.
- [11] S. S. Kalsi, K. Weeber, H. Takesue, C. Lewis, H. W. Neumueller, and R. D. Blaugher, "Development status of rotating machines employing superconducting field windings," *Proc. IEEE*, vol. 92, no. 10, pp. 1688–1695, Oct. 2004.